Comparison between Electric Field Analysis Methods Induced in Human Body by ELF Magnetic Field

Y. Takahashi[1], A. Ahagon[2], K. Fujiwara[1], T. Iwashita[3] and H. Nakashima[3]
[1] Doshisha University, 1-3 Tatara Miyakodani, Kyotanabe, Kyoto 610-0321 Japan
[2] Science Solutions International Laboratory, Inc., 2-21-7 Naka-cho, Meguro-ku, Tokyo 153-0065, Japan
[3] Kyoto University, Yoshida-Honmachi, Sakyo-ku, Kyoto 606-8501, Japan
ytakahashi@mail.doshisha.ac.jp

***Abstract*—This paper investigates effectiveness of a finite element method (FEM) and a boundary element method (BEM) in analysis of electric field induced in human body by extremely low frequency (ELF) magnetic field. The formulations of the FEM and BEM specialized for induced field analysis are presented and their features are discussed from the standpoints of accuracy and computational cost. Finally, the induced field analysis of anatomically-based human body model is carried out to demonstrate the effectiveness of the developed methods.**

***Index Terms*— Biomagnetics, Boundary element methods, Electromagnetic compatibility, Finite element methods, Parallel processing.**

I. Introduction

Recently, interest in electromagnetic environment and its adverse health effect is increasing drastically [1]. In order to evaluate the influence of static or time-varying electric and magnetic field, numeric anatomically-based human body model is widely used in each frequency band. In this paper, we focus on electric field induced in human body by extremely low frequency (ELF) magnetic field generated by home electric appliances and electric power equipment such as electric power line and electric substation equipment.

The effectiveness of various computational methods, for example the impedance method, scalar potential finite difference method, boundary element method (BEM), and quasi-static finite-difference time-domain method, has been reported in the induced field analysis [2]. In this paper, first we present the formulations of finite element method (FEM) and BEM specialized for induced field analyses and their features are discussed from the standpoints of computational accuracy and cost. The GPU-accelerated BEM with the fast multipole method (FMM) [3] for induced field calculation was investigated in detail in [4]. In this paper, its scalability in distributed computing environment using MPI programming for parallelization is examined. Finally, the induced field analysis of anatomically-based human model [5] is performed.

II. Method of Analysis

In the case where the conductivity of non-magnetic biomaterials is very small, the secondary magnetic field generated by induced current in the materials can be negligible compared with applied ELF magnetic field. Thus, the electric field $\boldsymbol{E}$ induced in human body satisfies

$$\nabla \times \boldsymbol{E} = -\frac{\partial \boldsymbol{B}_{\mathrm{a}}}{\partial t}, \tag{1}$$

where $\boldsymbol{B}_{\mathrm{a}}$ is the applied flux density. From (1), the continuity equation of current $\nabla \cdot \boldsymbol{J} = 0$ and the Ohm's law $\boldsymbol{J}=\sigma\boldsymbol{E}$, the basic equation of induced electric field in low frequency magnetic field is given by

$$\nabla \cdot \sigma\left(\frac{\partial \boldsymbol{A}_{\mathrm{a}}}{\partial t} + \nabla\phi\right) = 0, \tag{2}$$

where ϕ is electric scalar potential and $\boldsymbol{A}_{\mathrm{a}}$ is magnetic vector potential corresponding to $\boldsymbol{B}_{\mathrm{a}}$. In the finite element formulation, the Galerkin's weak form of (2) is obtained as

$$\int \nabla N \cdot \sigma \nabla\phi \,\mathrm{d}V = \int -\nabla N \cdot \sigma \frac{\partial \boldsymbol{A}_{\mathrm{a}}}{\partial t}\,\mathrm{d}V, \tag{3}$$

where N is the scalar shape function. This FEM formulation has advantages that mesh division for free space is unnecessary and it can treat materials with anisotropic conductivity such as skeletal muscle and represent arbitrary shape of organs, although the numeric human phantom is frequently composed of voxel data.

Next, we formulate the BEM for induced current analysis. At a surface between medium 1 and medium 2, the continuity of normal component of $\boldsymbol{J}$ is obtained as

$$\sigma_1 \boldsymbol{E}_1 \cdot \boldsymbol{n} = \sigma_1\left(\frac{\partial \boldsymbol{A}_{\mathrm{a}}}{\partial t} + \nabla\phi\right)\cdot\boldsymbol{n} = \sigma_2\left(\frac{\partial \boldsymbol{A}_{\mathrm{a}}}{\partial t} + \nabla\phi\right)\cdot\boldsymbol{n} = \sigma_2 \boldsymbol{E}_2 \cdot \boldsymbol{n}, \tag{4}$$

where $\boldsymbol{n}$ is the normal unit vector on interfacial boundary. When medium 1 and medium 2 have the same permittivity but different conductivity, the surface charge is induced on the interfacial boundary. As for a discretization method, we use the Galerkin's method for numerical stability. Finally, the following boundary integral equation is obtained:

$$\int_{S_i} \frac{(\sigma_1+\sigma_2)}{(\sigma_1-\sigma_2)}\frac{\sigma_{\mathrm{s}i}}{2}\mathrm{d}S_i - \sum_{j=1,j\neq i}^{NE}\int_{S_i}\int_{S_j} \frac{\sigma_{\mathrm{s}j}(\boldsymbol{r}_i-\boldsymbol{r}_j)\cdot\boldsymbol{n}_i}{4\pi|\boldsymbol{r}_i-\boldsymbol{r}_j|^3}\mathrm{d}S_i\mathrm{d}S_j = -\int_{S_i}\frac{\partial \boldsymbol{A}_{\mathrm{a}}}{\partial t}\cdot\boldsymbol{n}_i\mathrm{d}S_i \tag{5}$$

where NE is the number of unknowns and σ_{s} is the surface charge density. Equation (5) satisfies the continuity of total flux passing through each element. Because solving (5) requires very huge computational costs, we introduce the FMM and make the best use of regularity of voxel data [4]. The parallel efficiency of the BEM with the FMM is sufficiently good [6] even in highly parallel computation.

III. Numerical Examples

In order to verify the validity of the developed methods, we perform the induced field analysis of eccentric two spheres shown in Fig. 1 located in homogeneous magnetic field. Fig. 2(a) shows the comparison of induced electric fields along the y-axis. The calculated and theoretical values are different near region boundaries. This is because the shape representation of voxel data is not good microscopically as shown in Fig. 1(c). By applying smoothing based on weighted average to induced

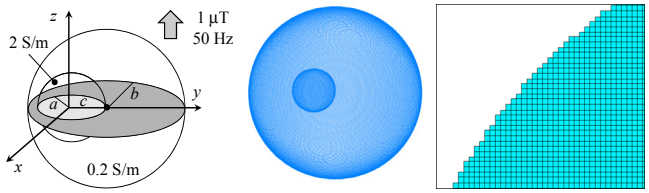

(a) (b) (c)

Fig. 1. Eccentric spheres model with two media. (a) Configuration of spheres. Radiuses of inner sphere a is 25 mm, that of outer sphere b is 100 mm, and the distance c between the centers of two spheres is 25 mm. (b) Voxel model (size = $1\times1\times1$ mm^3). (c) Cross-sectional view at $z = 0$ around region boundary.

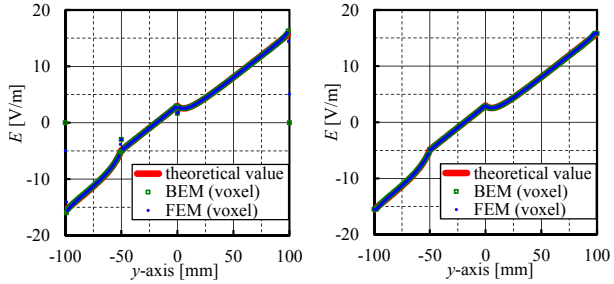

(a) (b)

Fig. 2. Numerical results of eccentric spheres. (a) Before smoothing. (b) After smoothing.

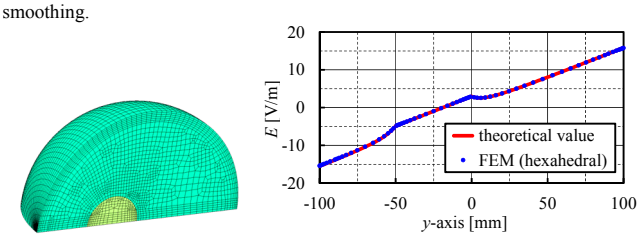

(a) (b)

Fig. 3. Numerical results of hexahedral mesh of eccentric spheres. (a) Finite element mesh (50,580 elements). (b) Comparison of induced fields.

fields near boundaries [7], the accuracy can be improved as indicated in Fig. 2(b). Because the use of hexahedral elements improves the shape representation as shown in Fig. 3(a), accurate results can be obtained from the FEM as shown in Fig. 3(b) regardless of the much smaller number of unknowns compared with its voxel model.

Next, we perform the induced field analysis of the anatomically-based human body model shown in Fig. 4(a), which consists of 7,977,906 voxels (voxel size = $2\times2\times2$ mm^3). We adopt the conductivities of each organ by reference to [2]. Figs. 4(b) and (c) show the distribution of induced electric field intensities when 1 μT is applied from foot to head at 50 Hz. The numerical results obtained from the FEM agree well with those obtained from the BEM. Table I shows the calculation time of sequential analyses by the FEM and BEM. In the case that the human body has homogeneous conductivity, the number of unknowns for the BEM is relatively small compared with the FEM. Thus, the BEM is faster than FEM. On the other hand, in the case that 50 organs are considered, the computational cost of the FEM is smaller than the BEM. Fig. 5 shows the parallel speedup over the sequential calculation. The developed method can achieve about 90-fold speedup when using 256 processes.

The detail of the formulations of the FEM and BEM specialized for induced field analysis, the parallelization method for the BEM with the FMM, and more numerical results will be included in the full paper.

TABLE I ANALYSIS RESULTS

	Eccentric spheres		Human body (homogeneous conductivity)		Human body (50 organs)	
	FEM	BEM	FEM	BEM	FEM	BEM
Number of unknowns	4,282,712	200,268	8,329,766	616,910	8,329,766	3,921,953
Calculation time [sec]	278.3	97.0	2,070.4	634.9	2,072.1	6,566.8

Used PC: Intel Core i7-975 Extreme Edition/3.33GHz for BEM and Intel Core i7-2600/3.40GHz for FEM

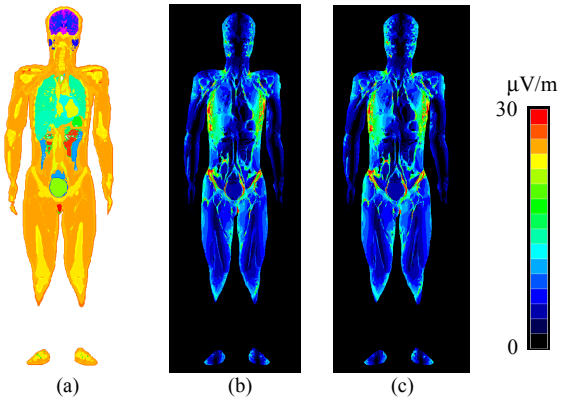

(a) (b) (c)

Fig. 4. Comparison of induced electric field intensities. (a) Numeric human body model. (b) Obtained from FEM. (c) Obtained from BEM.

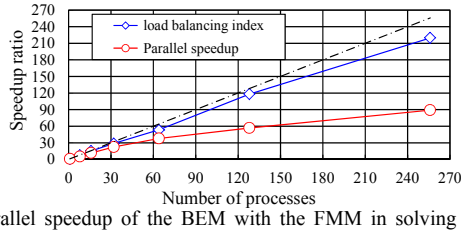

Fig. 5. Parallel speedup of the BEM with the FMM in solving (5). The computations were performed on the supercomputer Cray XE6, in which a node consists of two AMD Opteron6000 processors [8].

REFERENCES

[1] ICNIRP, "Guidelines for Limiting Exposure to Time-Varying Electric and Magnetic Fields (1 H - 100 kHz)", Health Physics 99(6):818-836; 2010.

[2] A. Hirata, K. Yamazaki, S. Hamada, Y. Kamimura, H. Tarao, K. Wake, Y. Suzuki, N. Hayashi, and O. Fujiwara, "Intercomparison of induced fields in Japanese male model for ELF magnetic field exposures: effect of different computational methods and codes," *Radiation Protection Dosimetry*, Vol. 138, No. 3, pp. 237-244, 2010.

[3] L. Greengard and V. Rokhlin, "A New Version of the Fast Multipole Method for the Laplace Equation in Three Dimensions," *Acta Numerica*, Vol.6, pp.229–269, 1997.

[4] S. Hamada, "GPU-accelerated indirect boundary element method for voxel model analyses with fast multipole method," *Computer Physics Communications*, vol. 182, no. 5, pp. 1162-1168, 2011.

[5] T. Nagaoka, S. Watanabe, K. Sakurai, E. Kunieda, S. Watanabe, M. Taki and Y. Yamanaka, "Development of Realistic High-Resolution Whole-Body Voxel Models of Japanese Adult Male and Female of Average Height and Weight, and Application of Models to Radio-Frequency Electromagnetic-Field Dosimetry," *Physics in Medicine and Biology*, Vol.49, pp.1-15, 2004.

[6] Y. Takahashi, T. Iwashita, H. Nakashima, S. Wakao, K. Fujiwara, and Y. Ishihara, "Performance Evaluation of Parallel Fast Multipole Accelerated Boundary Integral Equation Method in Electrostatic Field Analysis," *IEEE Trans. Magn.*, vol. 47, no. 5, pp. 1174-1177, 2011.

[7] S. Hamada and T. Kobayashi, "Analysis of Electric Field Distribution Induced by 50Hz Magnetic Fields Utilizing Fast-Multipole Surface-Charge-Simulation Method for Voxel Models," International Conference on Computational Methods, OW5-2, 2007.

[8] http://www.iimc.kyoto-u.ac.jp/en/services/comp/services/supercomputer.html